

## Supplementary Information

Persistence against benzalkonium chloride promotes rapid evolution of tolerance during periodic disinfection

Niclas Nordholt<sup>a#</sup>, Orestis Kanaris<sup>a</sup>, Selina B.I. Schmidt<sup>a</sup>, Frank Schreiber<sup>a#</sup>

<sup>a</sup>Division of Biodeterioration and Reference Organisms (4.1), Department of Materials and the Environment, Federal Institute for Materials Research and Testing (BAM), Berlin, Germany

<sup>#</sup>Address correspondence to Niclas Nordholt and Frank Schreiber, [niclas.nordholt@bam.de](mailto:niclas.nordholt@bam.de) and [frank.schreiber@bam.de](mailto:frank.schreiber@bam.de); Tel.: +49-30-8104-1414

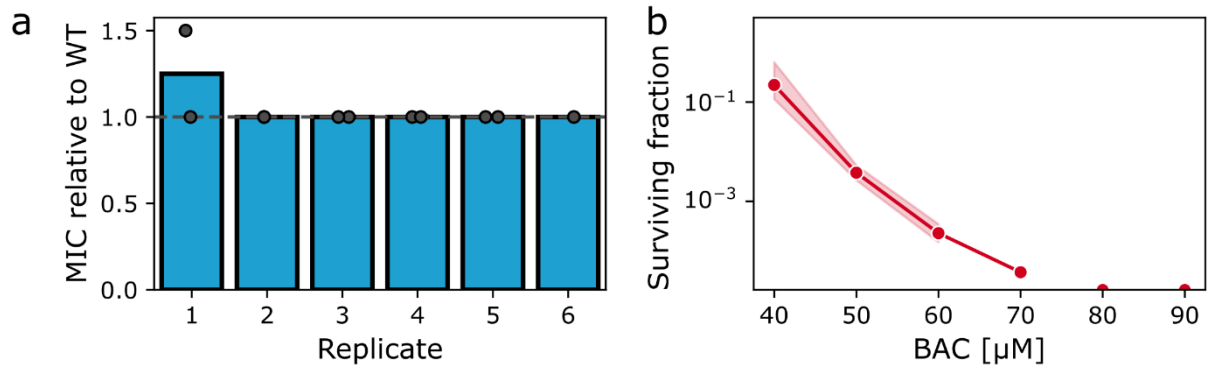


**Figure S1: a)** BAC persisters are not resistant mutants. *E. coli* was exposed to 60  $\mu$ M BAC. Per biological replicate, two colonies of surviving cells after 15 minutes of BAC treatment were picked and the MIC of BAC was determined. **b)** Concentration dependence of persisters after 20 minutes of BAC treatment (Spearman correlation coefficient -0.958,  $p = 2 \times 10^{-7}$ ,  $n = 3$  biological replicates. Data points show the geometric mean  $\pm$  95% confidence intervals. Significance of correlation: two-sided test with t-distribution of the test statistic). This figure accompanies figure 1. Source data are provided as a Source Data file.

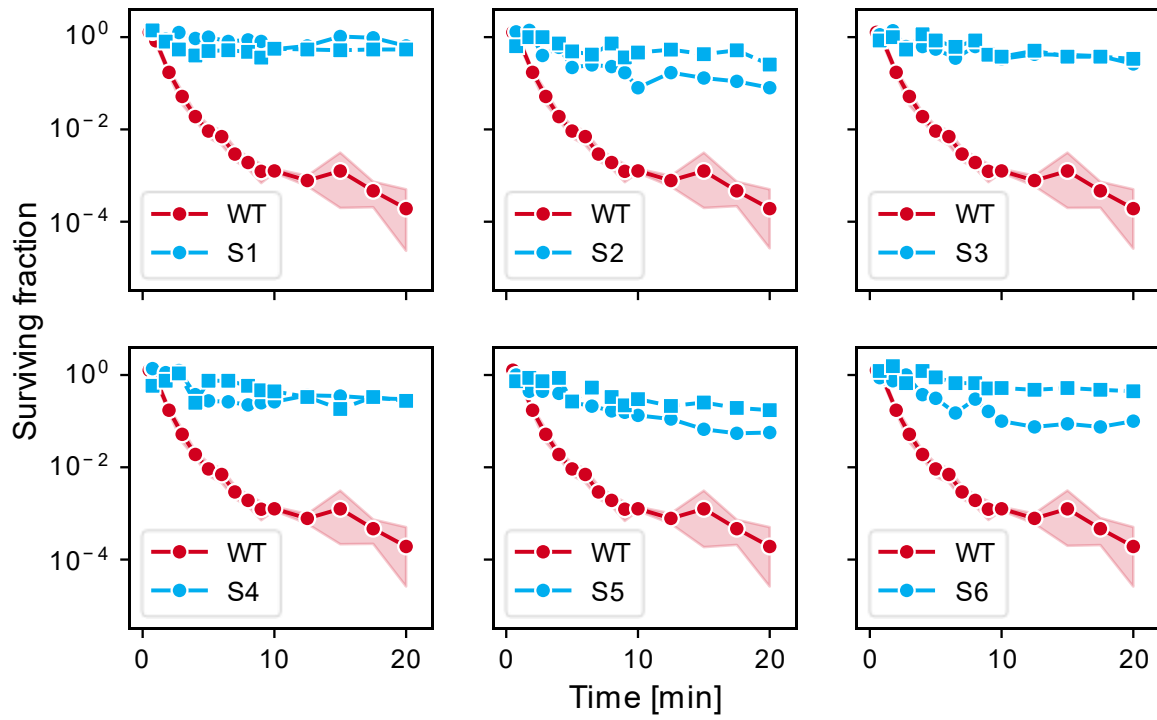


**Figure S2: Time-kill curves of evolved clones.** Blue symbols represent individual replicates of the surviving fraction ( $n=2$  biological replicates). For the wild-type (WT), the symbol represents the geometric mean and the shaded area represents the 95% confidence interval ( $n=6$  biological replicates). The red curve is the same as in figure 1 A in the main text. This figure accompanies figure 2. Source data are provided as a Source Data file.

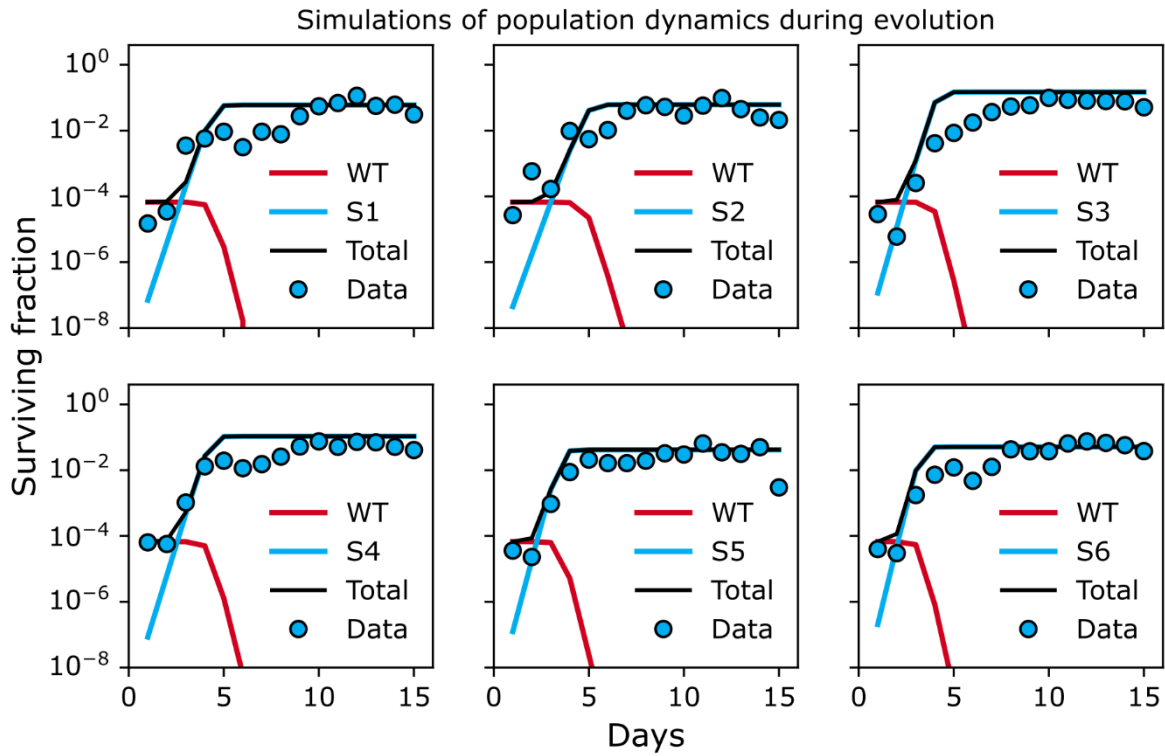


**Figure S3: Simulations of the population dynamics during evolution for all evolved clones.** Simulations of survival fraction during the serial passage experiment with alternating growth and kill cycles (lines) quantitatively reproduce the experimental data (circles). The parameters for growth rate and survival fraction are the same as in figure 2 C. Yield was inferred from cfu to  $OD_{600}$  conversion factors of the individual strains. Initial number of ancestor and mutant cells:  $10^5$  and 1 respectively. This figure accompanies figure 2. Source data are provided as a Source Data file.

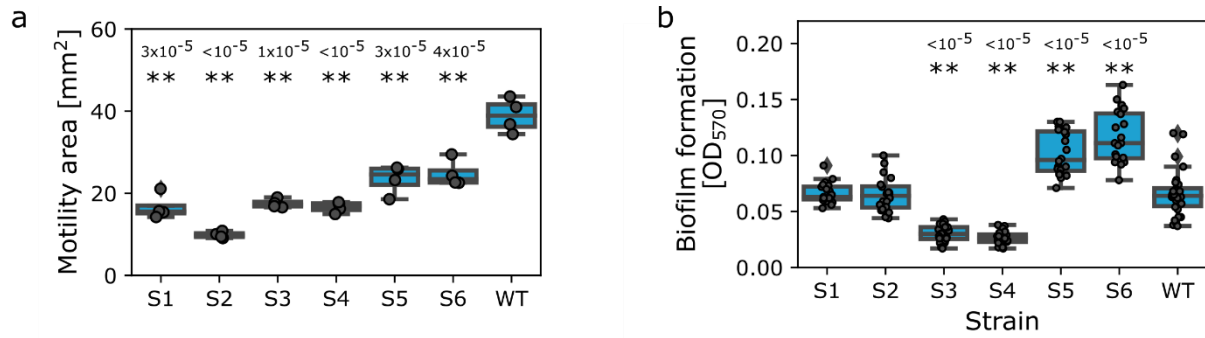


**Figure S4: Motility and biofilm formation are affected in the evolved clones.** **a)** Motility is decreased in all evolved clones. Boxes denote the interquartile range (IQR) between the first and third quartile, with the line showing the median. Whiskers indicate the minima and maxima of the data or have a length of 1.5 IQR if data fall outside the 1.5 IQR. n = 4 biological replicates. Significance of motility area against ancestor: \*, p < 0.05; \*\*, p < 0.01 (one-tailed t-test of motility area in mm<sup>2</sup>). **b)** Evolved BAC tolerance affects biofilm formation. Boxes denote the IQR, with the line showing the median. Whiskers indicate the minima and maxima of the data or have a length of 1.5 IQR if data fall outside the 1.5 IQR. n = 20 biological replicates. Significance of biofilm formation against the ancestor is indicated by asterisks: \*, p < 0.05; \*\*, p < 0.01 (two-tailed t-test of optical density at 570 nm). Exact p-values are indicated above the asterisks. Source data are provided as a Source Data file.

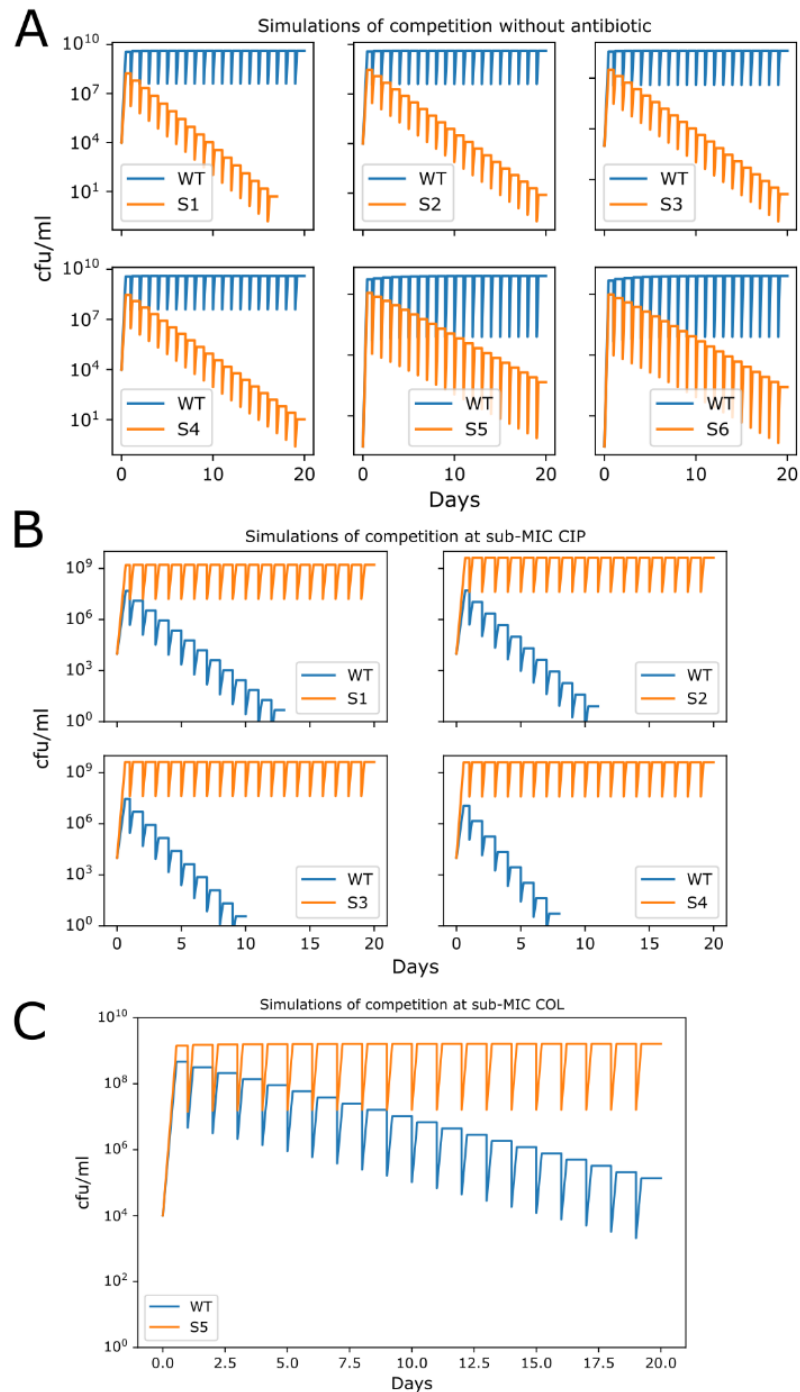


**Figure S5: Simulations of competition experiments in the absence and presence of sub-inhibitory antibiotic concentrations.** **A)** When competing in the absence of antibiotics, the wild-type wins over the evolved clones due to the costs of tolerance. **B)** In the presence of ciprofloxacin, four of the evolved clones outcompete the ancestor within 7 – 12 growth cycles. **C)** S5 outcompetes the wild-type in sub-inhibitory levels of colistin. Simulations are shown for strains with a growth-rate significantly different from the wild-type (see Figure 2C and Figure 5B in the main text). This figure accompanies figure 5 in the main text.

**Table S1: Mutations in all evolved clones generated in this study.**

Strain	Genomic position	Mutation	Amino acid substitution	Gene(s)	Annotation
<b>S1c1</b> S1c2	1,094,727	Δ26,518 bp	n.a.	<i>ymdE, ycdU, serX, ghrA, ycdX, ycdY, ycdZ, csgG, csgF, csgE, csgD, csgB, csgA, csgC, ymdA, ymdB, clsC, opgC, opgG, opgH, yceK, msyB, mdtG, lpxL, yceA, yceI, yceJ, yceO, solA, bssS, dinI, [pyrC]</i>	IS3-mediated See Table S2 for details
	1,939,467	G→A	intergenic (-50/+70)	<i>lpxM</i> ← / ← <i>mepM</i>	myristoyl-acyl carrier protein-dependent acyltransferase/peptidoglycan DD-endopeptidase MepM
<b>S2c1</b> S2c2	1,115,520	G→T	A96E	<i>lpxL</i> ←	lauroyl acyltransferase
	1,971,413	Δ6,314 bp	n.a.	<i>[tar], cheW, cheA, motB, motA, flhC, flhD</i>	IS1-mediated See Table S2 for details
<b>S3c1</b>	1,289,634	T→C	C57R	<i>rssB</i> →	regulator of RpoS
	1,938,693	G→T	A242E	<i>lpxM</i> ←	myristoyl-acyl carrier protein-dependent acyltransferase
S3c2	1,938,874	C→T	G182S	<i>lpxM</i> ←	myristoyl-acyl carrier protein-dependent acyltransferase
	1,967,842	Δ9,885 bp	n.a.	<i>[cheR], tap, tar, cheW, cheA, motB, motA, flhC, flhD</i>	IS1-mediated See Table S2 for details
S4c1	1,290,339	C→T	Q292*	<i>rssB</i> →	regulator of RpoS
	1,938,979	C→A	A147S	<i>lpxM</i> ←	myristoyl-acyl carrier protein-dependent acyltransferase
<b>S4c2</b>	1,290,339	C→T	Q292*	<i>rssB</i> →	regulator of RpoS
	1,938,975	A→C	M148R	<i>lpxM</i> ←	myristoyl-acyl carrier protein-dependent acyltransferase
<b>S5c1</b> S5c2	1,108,517	+9 bp	intergenic (-352/-34)	<i>opgC</i> ← / → <i>opgG</i>	protein required for succinyl modification of osmoregulated periplasmic glucans/osmoregulated periplasmic glucans (OPGs) biosynthesis protein G

	1,938,799	A→T	L207I	<i>lpxM</i> ←	myristoyl-acyl carrier protein-dependent acyltransferase
S6c1	1,111,908	Δ2 bp	coding (1822-1823/2544 nt)	<i>opgH</i> →	osmoregulated periplasmic glucans (OPGs) biosynthesis protein H
	1,938,526	A→C	W298G	<i>lpxM</i> ←	myristoyl-acyl carrier protein-dependent acyltransferase
	4,123,417	Δ13 bp	<i>intergenic</i> (-78/+2)	<i>ftsN</i> ← / ← <i>cytR</i>	<i>cell division protein FtsN/DNA-binding transcriptional repressor CytR</i>
<b>S6c2</b>	1,111,908	Δ2 bp	coding (1822-1823/2544 nt)	<i>opgH</i> →	osmoregulated periplasmic glucans (OPGs) biosynthesis protein H
	1,938,526	A→C	W298G	<i>lpxM</i> ←	myristoyl-acyl carrier protein-dependent acyltransferase

n.a., not applicable; bold typeface indicates clones selected for further analyses in the main text; italic font indicates rare mutations that were not present in the population sequencing approach

**Table S2: Genes affected by large IS-mediated deletions.**

Clone	Gene	Annotation
S1	<i>ymdE</i>	Uncharacterized protein YmdE
	<i>ycdU</i>	Uncharacterized protein YcdU
	<i>serX</i>	tRNA-Ser
	<i>ghrA</i>	glyoxylate/hydroxypyruvate reductase A
	<i>ycdX</i>	zinc-binding phosphatase
	<i>ycdY</i>	chaperone protein YcdY
	<i>ycdZ</i>	putative inner membrane protein
	<i>csgG</i>	curli secretion channel
	<i>csgF</i>	curli assembly component
	<i>csgE</i>	curli transport specificity factor
	<i>csgD</i>	DNA-binding transcriptional dual regulator CsgD
	<i>csgB</i>	curlin minor subunit
	<i>csgA</i>	curlin major subunit
	<i>csgC</i>	inhibitor of CsgA amyloid formation
	<i>ymdA</i>	uncharacterized protein YmdA
	<i>ymdB</i>	2'-O-acetyl-ADP-ribose deacetylase regulator of RNase III activity
	<i>clsC</i>	cardiolipin synthase C
	<i>opgC</i>	protein required for succinyl modification of osmoregulated periplasmic glucans
	<i>opgG</i>	osmoregulated periplasmic glucans (OPGs) biosynthesis protein G
	<i>opgH</i>	osmoregulated periplasmic glucans (OPGs) biosynthesis protein H
	<i>yceK</i>	DUF1375 domain-containing lipoprotein YceK
	<i>msyB</i>	acidic protein that suppresses heat sensitivity of a <i>secY</i> mutant
	<i>mdtG</i>	efflux pump MdtG
	<i>lpxL</i>	lauroyl acyltransferase
	<i>yceA</i>	UPF0176 protein YceA
	<i>yceI</i>	Uncharacterized protein YceI
	<i>yceJ</i>	putative cytochrome b561
	<i>yceO</i>	DUF2770 domain-containing protein YceO
	<i>sola</i>	N-methyl-L-tryptophan oxidase
	<i>bssS</i>	regulator of biofilm formation
<i>dinI</i>	DNA damage-inducible protein I	
<i>pyrC</i>	dihydroorotase	
S2	<i>tar</i>	methyl-accepting chemotaxis protein Tar
	<i>cheW</i>	chemotaxis protein CheW
	<i>cheA</i>	chemotaxis protein CheA
	<i>motB</i>	motility protein B
	<i>motA</i>	motility protein A
	<i>flhC</i>	DNA-binding transcriptional dual regulator FlhC
	<i>flhD</i>	DNA-binding transcriptional dual regulator FlhD
S3c2	<i>cheR</i>	chemotaxis protein methyltransferase
	<i>tap</i>	methyl-accepting chemotaxis protein Tap
	<i>tar</i>	methyl-accepting chemotaxis protein Tar
	<i>cheW</i>	chemotaxis protein CheW
	<i>cheA</i>	chemotaxis protein CheA
	<i>motB</i>	motility protein B
	<i>motA</i>	motility protein A
	<i>flhC</i>	DNA-binding transcriptional dual regulator FlhC
<i>flhD</i>	DNA-binding transcriptional dual regulator FlhD	

**Table S3: Bacterial strains used in this study.**

Designation in main text	Designation in original publication	Description	Genotype	Source, Citation
MG1655 (wild-type)	K-12 MG1655	Wild type	$\Delta 776$ bp insB9-[crl], +8 bp bamD $\rightarrow / \rightarrow$ raiA, +GC gltP $\rightarrow / \leftarrow$ yjcO compared to NC_000913.3	R. Mutzel lab <sup>1</sup>
$\Delta tolC$	TB283	Knock-out of the multi-drug efflux channel <i>tolC</i>	MG1655 <i>attP21::PR-mCherry::frrt</i> <i>\Delta tolC::FRT</i>	C. Guet lab <sup>2</sup>
$\Delta relA spoT$	$\Delta relA \Delta spoT$	Double knockout of the (p)ppGpp synthase/hydrolase <i>relA spoT</i>	MG 1655 <i>\Delta relA::frrt</i> <i>\Delta spoT::frrt</i>	K. Lewis lab <sup>3</sup>
$P_{lac}$ - <i>marA</i>	<i>MarA</i> -CFP	Multi-antibiotic resistance transcription factor <i>marA</i> under control of an IPTG-inducible promoter	MG1655 pBbA5k <i>marA</i> -CFP	M. Dunlop lab <sup>4</sup>
$\Delta marRAB$	$\Delta marRAB$	Knockout of the <i>marRAB</i> operon. Contains a low copy plasmid with CFP under the control of the <i>marA</i> promoter.	MG1655 $\Delta marRAB$ pBbSVk- $P_{marA}$ -CFP	M. Dunlop lab <sup>4</sup>
$P_{lac}$ - <i>tisB</i>	pZS*24 <i>tisB</i>	Persistence-inducing toxin <i>tisB</i> under control of an IPTG-inducible promoter	MG1655 pZS*24 <i>tisB</i>	K. Lewis lab <sup>5</sup>
$P_{BAD}$ - <i>hokB</i>	PBAD/ <i>HisA-hokB</i>	Persistence-inducing toxin <i>hokB</i> under control of an arabinose-inducible promoter	MG1655 PBAD/ <i>HisA-hokB</i>	J. Michiels lab <sup>6</sup>
$\Delta fliC$	TB205	Knock-out of the flagellin gene <i>fliC</i>	MG1655 <i>attP21::PR-mCherry::FRT</i> <i>\Delta fliC::FRT</i>	C. Guet lab <sup>2</sup>
$P_{lac}$ - <i>lpxM</i>	JW1844-AM	Lipid A biosynthesis myristoyltransferase <i>lpxM</i> under control of an IPTG-inducible promoter	MG1655 pCA24N-Plac/T5_6His- <i>lpxM</i>	ASKA collection <sup>7</sup>
$P_{lac}$ - <i>rpoE</i>	JW2557-AM	Envelope-stress sigma factor <i>rpoE</i> under control of an IPTG-inducible promoter	MG1655 pCA24N-Plac/T5_6His- <i>rpoE</i>	ASKA collection <sup>7</sup>
$\Delta lpxM$	BW25113 <i>lpxM::FRT-Kan-FRT</i>	Knock-out of lipid A biosynthesis myristoyltransferase <i>lpxM</i>	BW25113 <i>lpxM::FRT-Kan-FRT</i>	Keio collection <sup>8</sup>

**Table S3: Bacterial strains used in this study.**

<b>Designation in main text</b>	<b>Designation in original publication</b>	<b>Description</b>	<b>Genotype</b>	<b>Source, Citation</b>
BW25113 (wild-type)	BW25113		<i>rrnB3 ΔlacZ4787</i> <i>hsdR514</i> <i>Δ(araBAD)567</i> <i>Δ(rhaBAD)568 rph-1.</i>	Keio collection <sup>8</sup>

## References

1. Blattner, F. R. *et al.* The complete genome sequence of *Escherichia coli* K-12. *Science* **277**, 1453–1462 (1997).
2. Bergmiller, T. *et al.* Biased partitioning of the multidrug efflux pump AcrAB-TolC underlies long-lived phenotypic heterogeneity. *Science* **356**, 311–315 (2017).
3. Shan, Y. *et al.* ATP-Dependent persister formation in *Escherichia coli*. *mBio* **8**, e02267-16 (2017).
4. Meouche, I. E., Siu, Y. & Dunlop, M. J. Stochastic expression of a multiple antibiotic resistance activator confers transient resistance in single cells. *Sci. Rep.* **6**, 1–9 (2016).
5. Dörr, T., Vulić, M. & Lewis, K. Ciprofloxacin causes persister formation by inducing the TisB toxin in *Escherichia coli*. *PLoS Biol.* **8**, e1000317 (2010).
6. Verstraeten, N. *et al.* O<sub>bg</sub> and Membrane Depolarization Are Part of a Microbial Bet-Hedging Strategy that Leads to Antibiotic Tolerance. *Mol. Cell* **59**, 9–21 (2015).
7. Kitagawa, M. *et al.* Complete set of ORF clones of *Escherichia coli* ASKA library ( A Complete Set of *E. coli* K-12 ORF Archive): Unique Resources for Biological Research. *DNA Res.* **12**, 291–299 (2005).
8. Baba, T. *et al.* Construction of *Escherichia coli* K-12 in-frame, single-gene knockout mutants: the Keio collection. *Mol. Syst. Biol.* **2**, 2006.0008 (2006).